



Unusual liver tumors: spectrum of imaging findings with pathologic correlation

Nir Stanietzky¹
 Ahmed Ebada Salem^{2,3}
 Khaled M. Elsayes¹
 Maryam Rezvani²
 Sarah Palmquist¹
 Imran Ahmed¹
 Ahmed Marey³
 Silvana Faria¹
 Ayman H. Gaballah¹
 Christine O. Menias⁴
 Akram M. Shaaban²

¹University of Texas MD Anderson Cancer Center, Department of Radiology, Texas, USA

²The University of Utah, Department of Radiology, Utah, USA

³Alexandria University Faculty of Medicine, Department of Radiodiagnosis and Intervention, Alexandria, Egypt

⁴Mayo Clinic, Department of Radiology, Arizona, USA

ABSTRACT

The liver is a common location for both primary and secondary cancers of the abdomen. Radiologists become familiar with the typical imaging features of common benign and malignant liver tumors; however, many types of liver tumors are encountered infrequently. Due to the rarity of these lesions, their typical imaging patterns may not be easily recognized, meaning their underlying pathologic features may not be discovered or suggested until an invasive biopsy is performed. In this review article, we discuss multiple hepatic neoplasms that are both unusual and rare. Some have typical imaging patterns, whereas others are non-specific and can only be included in the differential diagnosis. The clinical history and serologic findings are often critical in suggesting these entities; therefore, these are also discussed to familiarize the radiologist with the appropriate clinical setting of each. The article includes an image-rich description of each entity with accompanying figures describing the ultrasonography, computed tomography, and magnetic resonance imaging features of each disease process. Novel therapies and prognosis of several of the diseases are also included in the discussion.

KEYWORDS

Clinical context, differential diagnosis, hepatic neoplasms, imaging features, pathologic correlation

Radiologists who are unfamiliar with the many etiologies of unusual hepatic tumors may misinterpret these lesions. Some present with unique imaging features, whereas others present in a similar fashion to common neoplasms. This article will serve as a useful reference for both general and subspecialized radiologists when encountering such lesions.

Primary hepatic neuroendocrine tumors

Intrabdominal neuroendocrine tumors (NET) typically originate from the gastrointestinal tract, specifically the appendix, ileum, and rectum. The liver is a common site for NET metastases; however, primary hepatic neuroendocrine tumors (PHNETs) are extremely rare and are believed to arise either from ectopic pancreatic cells or stem cells in the liver. As PHNETs are usually slow growing, they are typically discovered incidentally.¹ The most common ages of presentation are 40–50 years, and the tumor tends to be hormonally inactive, with non-specific clinical symptoms, ranging from asymptomatic to abdominal pain.² If hormonal symptoms occur, the patient typically demonstrates carcinoid syndrome or Cushing syndrome.

On imaging, PHNET presents as a large mixed cystic and solid lesion with surrounding satellite nodules. The solid component often demonstrates a hypervascular enhancement on the arterial phase, more so in the periphery, with delayed enhancement centrally (Figure 1). On magnetic resonance imaging (MRI), there is hyperintense T2 weighted signal and marked restriction on diffusion-weighted imaging (DWI).³ The tumor can produce tumor thrombus,¹ and can be confused with other arterially enhancing lesions, such as hepatocellular carcinomas (HCCs). However, PHNETs do not tend to occur in patients with cirrhosis or chronic liver disease.

Corresponding author: Khaled M. Elsayes

E-mail: kmelsayes@mdanderson.org

Received 25 April 2024; revision requested 12 May 2024; accepted 18 May 2024.



Epub: 10.06.2024

Publication date: xx.xx.2024

DOI: 10.4274/dir.2024.242827

Depending on the tumor grade differentiation and Ki-67 proliferation index, these lesions may demonstrate uptake on fluorodeoxyglucose (^{18}F -FDG)-positron emission tomography (PET)/computed tomography (CT). Low-grade tumors are typically hypometabolic, whereas grade 2 tumors can be hypo- or hypermetabolic. In contrast, grade 3, poorly differentiated neuroendocrine neoplasms are typically ^{18}F -FDG-PET/CT avid. Gallium-68-DOTA-somatostatin analogue-PET/CT and Indium-111 octreotide scanning, which are specific receptor imaging techniques, demonstrate a higher positive imaging rate for grade 1 and grade 2 tumors.⁴

No global consensus on the treatment of these lesions exists. Surgical resection is the treatment of choice, with a reported 10-year survival rate of 68%.^{1,4} For patients demonstrating recurrence or who are not eligible for surgery, transcatheter chemoembolization can be used, with a 5-year survival rate of 74%–78%.¹ Other treatment options include yttrium-90- and lutetium-177-labelled peptides. There is limited data on the effect of chemotherapy on the treatment and prognosis of PHNETs.¹

Extrapulmonary small cell carcinoma

The lung is the most common site of small cell carcinoma (SCC). Extrapulmonary SCC (EPSCC) usually occurs in the gastrointestinal tract and accounts for only 2.5%–5.0% of SCC,² with around 1,000 cases diagnosed in the United States per year. Both EPSCC and small cell lung cancer (SCLC) share some histopathologic features with NETs; EPSCC demonstrates a slight male predominance and presents at a mean age of 64, approximately 5–10 years earlier than SCC of the lung. The proportion of patients with EPSCC who smoke is lower than in SCC of the lung.⁵ These extrapulmonary tumors typically appear as a large, heterogeneous mass with non-specific imaging findings, and are indistinguishable from other common hepatic

neoplasms (Figure 2).⁶ Once hepatic EPSCC is diagnosed through biopsy, an extensive diagnostic workup including chest CT, PET/CT, and bronchoscopy is critical to exclude an extrahepatic primary site. As the liver is also the most common site of metastatic disease in other forms of EPSCC, determining the site of primary disease can be challenging when more than one organ is involved.⁵

The management of EPSCC is extrapolated from the treatment of SCLC due to the similar histologic features. However, this approach has limited evidence-based data.⁵ As with other NETs, the Ki-67 proliferation index is used to determine the grade. Unlike many other neuroendocrine neoplasms, EPSCC does not show a direct correlation between grade and aggressiveness; in fact, one study showed a higher number of metastases in tumors with a lower Ki-67 index.⁵ The response rate to chemotherapy is higher than that of SCLC. Of all the types of EPSCC, those originating in the gastrointestinal tract have the poorest 3-year survival rate (7% vs. an overall rate of 28%).⁵

Undifferentiated embryonal sarcoma

Undifferentiated embryonal sarcoma (UES) is a rare, highly aggressive malignant tumor of mesenchymal origin most commonly affecting children aged 6–10, with a slight male predominance.^{7,8} Although this tumor is rare, it is the third most common primary hepatic tumor in children after hepatoblastoma and HCC. This tumor is typically asymptomatic in children and can present with abdominal pain and fever in adults. Rarely, patients may present with an acute abdomen due to tumor rupture. In contrast to other pediatric liver tumors, such as hepatoblastoma and HCC, UES usually presents with normal alpha-fetoprotein levels, whereas hepatoblastoma presents with elevated alpha-fetoprotein levels in 95% of cases. The most common sites of UES metastasis are the lung, pleura, and peritoneum.⁸

On imaging, the UES tumor has a predilection for the right hepatic lobe, is large (approx. 10–29 cm), and is predominantly cystic in appearance due to the high water content of its myxoid stroma. Post-contrast imaging shows progressive delayed enhancement of

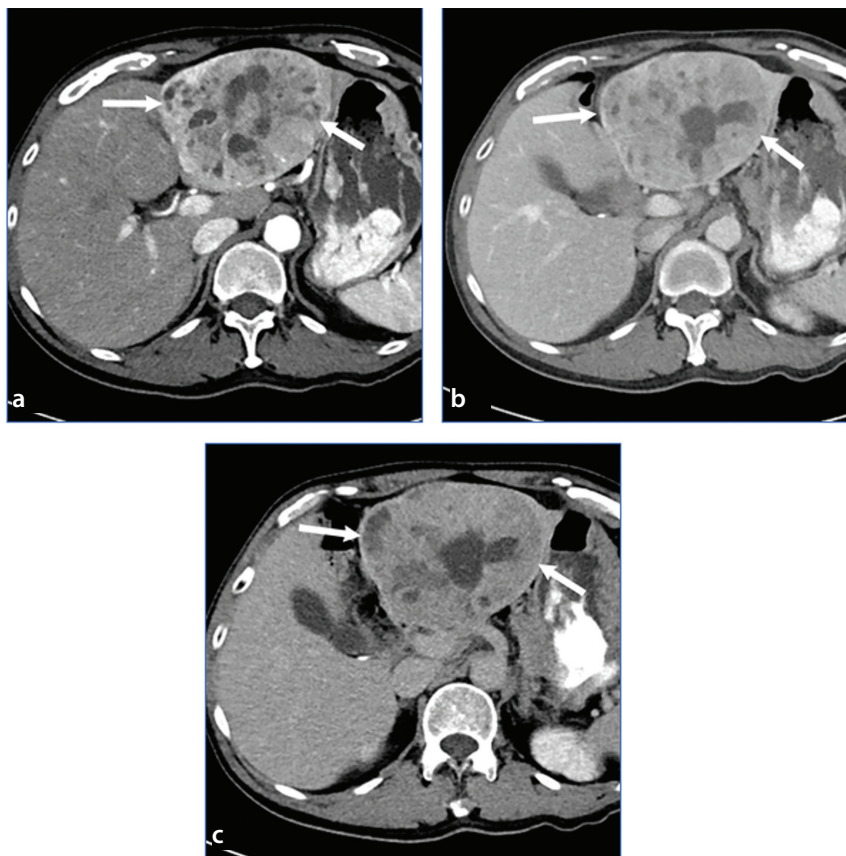


Figure 1. Primary hepatic neuroendocrine tumor. Axial contrast-enhanced computed tomography images of the liver during late arterial (a), portal venous (b), and delayed (c) phases of contrast enhancement show a round, heterogeneously enhancing primary hepatic neuroendocrine tumor replacing the lateral segments of the left lobe of the liver (arrows). The mass demonstrates increased enhancement during the arterial phase (particularly peripherally), washout of contrast material during the portal phase, and increased enhancement on the delayed phase as compared with the surrounding liver parenchyma.

Main points

- Unusual hepatic tumors are infrequently seen and it is therefore important for radiologists to be familiar with their imaging findings.
- While the imaging findings of many of these unusual tumors are non-specific, familiarity with these disease entities allows for their inclusion in the differential diagnosis.
- The clinical features of these entities are also described to aid in the differential diagnosis.

a thick peripheral rim, which corresponds to a fibrous pseudo capsule.⁸ CT demonstrates a fluid attenuating mass with thick peripheral rim of soft tissue. Calcifications are not typically present. Obtaining a delayed phase can aid in making an accurate diagnosis since delayed enhancement would not be seen in a simple hepatic cyst.⁷

Moreover, MRI shows a predominantly cystic-appearing mass with similar signal intensity to cerebrospinal fluid and a thick rim with low signal and delayed enhancement on both T1- and T2-weighted imaging, corresponding to the fibrous pseudocapsule (Figure 3). The tumor may contain focal areas of hyperintense signal on T1-weighted images, correlating to areas of intratumoral hemorrhage.⁸

Ultrasonography typically shows a solid isoechoic to hyperechoic mass relative to the background liver with varying degrees of anechoic regions, which correspond to internal necrosis and cystic degeneration.⁸ A cystic-appearing mass on CT and MRI that appears solid on ultrasonography favors the diagnosis of UES.

The differential diagnosis includes mesenchymal hamartoma of the liver, which can be difficult to distinguish from UES on pathology and imaging. The age of presentation can help guide the diagnosis, as UES is rare in children under 5 years, whereas mesenchymal hamartoma of the liver typically presents by 2 years. Due to its predominantly cystic appearance on cross-sectional imaging, UES can easily be misdiagnosed as a hydatid cyst or abscess. Thorough clinical

workup to look for peripheral eosinophilia seen with hydatid cysts and signs of infection seen with abscesses can aid in proper diagnosis.⁸ Treatment consists of multiagent chemotherapy followed by surgery in cases amenable to resection.⁷

Angiomyolipoma

Hepatic angiomyolipomas (AMLs) are rare, benign, mesenchymal tumors that consist of blood vessels, smooth muscle, and fat elements, and are more frequent in women and non-cirrhotic livers; AMLs more commonly occur in the kidneys and rarely involve the liver. An AML is associated with tuberous sclerosis in 20% of renal cases but only 6% of hepatic cases.⁹ In most cases, patients are asymptomatic, and their hepatic AML is discovered incidentally. The imaging appearance varies depending on the degree of fat composition. The fat content is variable, ranging from 90% to barely detectable.¹⁰ Other hepatic lesions can also contain fat, such as hepatic adenoma, HCC and, rarely, focal nodular hyperplasia.¹⁰ Definitive diagnosis is based on pathologic evaluation of the smooth muscle component and positive staining for homatropine methyl bromide-45 and smooth muscle markers.¹¹

On ultrasonography, hepatic AML appears highly echogenic and is indistinguishable from hemangioma (Figure 4). For lipid-rich AML, MRI evaluation demonstrates hyperintense signal on T1-weighted images with signal loss on fat suppression sequences, consistent with macroscopic fat. Distinguishing hepatic AML from HCC through imaging can be challenging. Some helpful AML features include isointensity on the portal venous phase, early draining veins, and intratumoral vessels. In addition, HCC frequently demonstrates restricted diffusion and a tumor capsule.¹⁰ A small percentage (4%) of the epithelioid subtype of hepatic AML can demonstrate malignant behavior with local invasion, recurrence after resection, and metastasis.¹¹

Angiosarcoma

Hepatic angiosarcoma is a malignant tumor that is extremely rare overall but is the most common hepatic mesenchymal tumor and has an extremely poor prognosis. It is more commonly seen in elderly men, and approximately one-fourth of cases are associated with exposure to thorium dioxide (Thorotrast) and vinyl chloride.

Clinically, patients typically present with hepatomegaly and other non-specific symp-

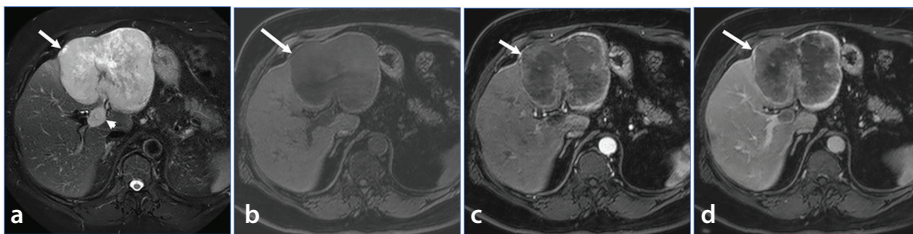


Figure 2. Extrapulmonary small cell carcinoma. Axial T2-weighted magnetic resonance imaging (MRI) with fat suppression (a) and pre-contrast (b) and dynamic post-gadolinium T1-weighted MRI with fat suppression in the arterial (c) and portal venous (d) phases show an extrapulmonary small cell carcinoma of the left hepatic lobe (white arrows) demonstrating high T2 signal intensity, low T1 signal intensity, and intense peripheral enhancement and poor central enhancement, with invasion of the left portal vein (short white arrow).

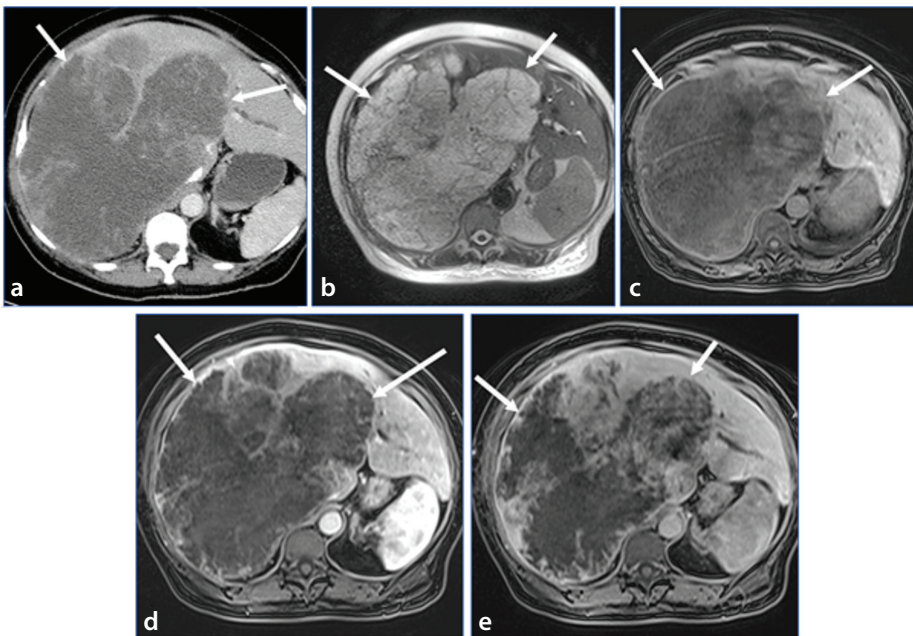


Figure 3. Undifferentiated embryonal sarcoma. Axial contrast-enhanced computed tomography (a) demonstrates a large predominantly cystic mass involving most of the right and part of the left hepatic lobe. Axial T2-weighted imaging (b) shows high signal intensity of the tumor, giving a cystic appearance. Axial dynamic gadolinium-enhanced T1-weighted imaging (c-e) show gradual contrast accumulation, revealing the solid nature of the tumor. This was pathologically proven to be embryonal sarcoma with possible cartilaginous differentiation.

toms, such as abdominal pain, weight loss, and fatigue. The median survival is poor at just 6 months.¹² Large angiosarcomas can cause hematologic abnormalities, such as disseminated intravascular coagulation, thrombocytopenia, and microangiopathic hemolytic anemia. Metastasis is common at initial diagnosis, most commonly involving the spleen and lungs. Approximately 15%–27% of patients may present with acute abdominal pain and anemia due to tumor rupture and hemoperitoneum.⁸ It is critical to be aware of potential massive hemorrhage as a complication of biopsy.

The tumor morphology of hepatic angiosarcoma can vary in appearance on imaging, showing multiple nodules/masses, a large dominant mass, or a diffuse infiltrative pattern (Figure 5). Intratumoral hemorrhage and necrosis are often present. On non-contrast CT, the tumor is hypoattenuating compared with normal background liver, with internal foci of hyperattenuation corresponding to hemorrhage. Contrast-enhanced CT shows intense peripheral nodular enhancement and can resemble a cavernous hemangioma but will not follow the blood pool on all phases and will generally not feature the true peripheral nodular discontinuous enhancement that is common in a cavernous hemangioma. More frequently, the tumor will appear hypodense on both arterial and portal venous phases with foci of early heterogeneous enhancement, occasionally with a central or ring pattern, but to a lesser degree than the aorta. On delayed phases, the tumor shows persistent enhancement, but the complete centripetal fill-in seen in hemangiomas is absent.

On MRI, the tumor is predominantly hypointense on T1-weighted images with internal foci of hyperintensity corresponding to intratumoral hemorrhage. On T2-weighted images, the tumor is generally heterogeneously hyperintense compared with background liver and may contain septa or fluid–fluid levels related to hemorrhage.^{8,13} Metastasis is common, affecting up to 60% of patients, and most commonly involves the lungs and spleen.⁸ It is critical to assess the dependent areas of the abdomen and pelvis to check for hemoperitoneum in cases of tumor rupture. The treatment of these lesions includes surveillance or surgical resection and liver transplant in unresectable cases.¹³

Epithelioid hemangioendothelioma

Hepatic epithelioid hemangioendothelioma (HEHE) is an extremely rare malignant

vascular tumor that typically presents in individuals in their 40s, more commonly in women, and the typical presentation includes abdominal pain, jaundice, and hepatosplenomegaly.¹⁴ Involvement of other organs has been observed in 36.6% of patients, most often affecting lungs, regional lymph nodes, and peritoneum, with bones frequently affected.¹⁵ A HEHE can mimic other tumors,

most commonly cholangiocarcinoma, HCC, metastatic carcinoma, and angiosarcoma. Definitive diagnosis requires pathologic assessment, which shows endothelial cells, identifiable by positive staining with antibodies against factor VIII, CD31, and CD34.¹⁶

Imaging features of HEHE demonstrate multiple hypoattenuating nodules on

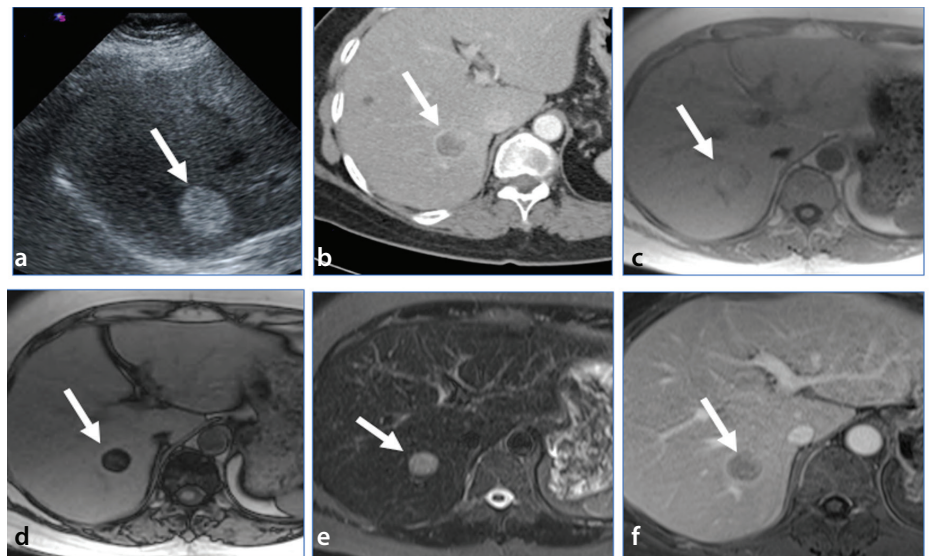


Figure 4. Angiomyolipoma. Transabdominal ultrasonography (a) shows a round echogenic mass (white arrow). Axial contrast-enhanced CT (b) shows a round, peripherally enhancing mass with poor central enhancement. Axial T1-weighted in-phase (c) and opposed-phase (d), axial T2-weighted (e), and post-gadolinium T1-weighted magnetic resonance images with fat suppression (f) show a round liver mass demonstrating loss of signal on opposed-phase images, high signal intensity on T2-weighted images, and rim enhancement following contrast administration.

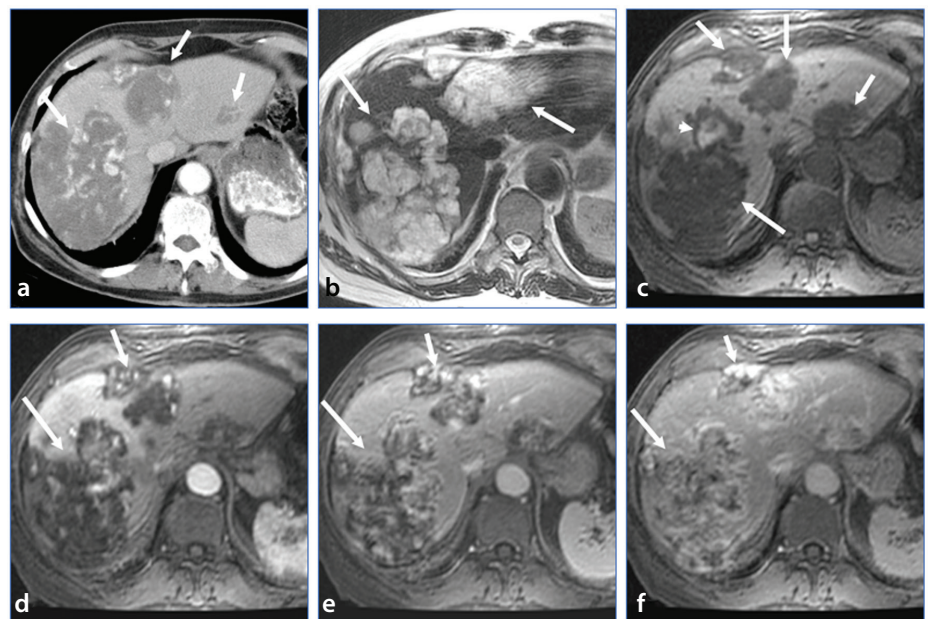


Figure 5. Angiosarcoma. Axial contrast-enhanced computed tomography (CT) (a), axial T2-weighted magnetic resonance imaging (MRI) (b), axial T1-weighted MRI (c), and dynamic post-gadolinium T1-weighted MRI with fat suppression (d-f) show multifocal liver angiosarcomas (long arrows). The masses demonstrate low attenuation relative to the liver on contrast-enhanced CT, high T2 signal intensity, low T1 signal intensity, and progressive enhancement following contrast administration. Early arterial enhancement is irregular and more central than in hemangiomas. High signal intensity within the lesion on T1-weighted imaging is due to hemorrhage. The T2 signal intensity is more heterogeneous than seen in hemangiomas.

non-contrast CT, which may or may not have calcifications. This tumor is most commonly subcapsular and can cause capsular retraction. Depending on the size of the lesion, these neoplasms can exhibit different patterns of contrast enhancement. Small lesions tend to demonstrate mild homogeneous enhancement; medium-size lesions can demonstrate ring enhancement, usually due to central necrosis; and large lesions demonstrate heterogeneous delayed enhancement.¹⁷ Also helpful in the diagnosis are a “halo” sign and a “lollipop” sign, which show a branch of a hepatic vein draining the tumor.¹⁸ Tumor thrombi may be present in the inferior vena cava.¹⁹ Multiple lesions are more likely to occur in HEHE than other, more common hepatic tumors such as HCC, intrahepatic cholangiocarcinoma, and hepatic metastases (Figure 6).¹⁵ However, as HEHE is a rare entity, multifocal liver masses are still more likely to represent these more common etiologies.

On MRI, HEHE tumors are typically T1 hypointense, heterogeneously T2 hyperintense, and diffusion restricting.²⁰ Ring enhancement is observed following intravenous contrast administration.²¹ Relatively specific MRI features of HEHE are capsular retraction, lollipop sign, and “target” sign on both T2-weighted and portal phase imaging (Figure 7).²⁰

On analysis with contrast-enhanced ultrasonography, HEHE demonstrates slower enhancement and more rapid washout time than more common hepatic tumors.²² Moreover, HEHE can easily be misdiagnosed as hepatic metastases on ultrasonography given the common presentation of multiplicity and hypoechoic appearance.²³ Therefore, cross-sectional imaging is key for further evaluation.

Surgery is the treatment of choice for a confirmed case of unifocal HEHE and should be performed in centers with sarcoma surgery experience. There are no definitive guidelines for treating multifocal HEHE or metastatic EHE, and these cases are treated with a combination of chemotherapy, radiation therapy, surgery, and liver transplant.²⁴

Hepatic schwannoma

Schwannomas (also called neurilemmomas) are benign, slow-growing nerve sheath tumors that typically occur in the head, neck, and upper extremities. These lesions can occur in all ages but are most common in women aged 20–50. Liver involvement of schwannomas is exceedingly uncommon,

and when it occurs, it most often presents in patients with neurofibromatosis type 1 [50% of cases (25)] or following radiation. Hepatic schwannomas are believed to originate from nerve fibers that themselves originate from

the plexus at the hepatic hilum. These fibers then branch out into the connective tissue along portal arteries and veins.²⁵

On imaging, hepatic schwannomas demonstrate T1 hypointensity and T2 hy-

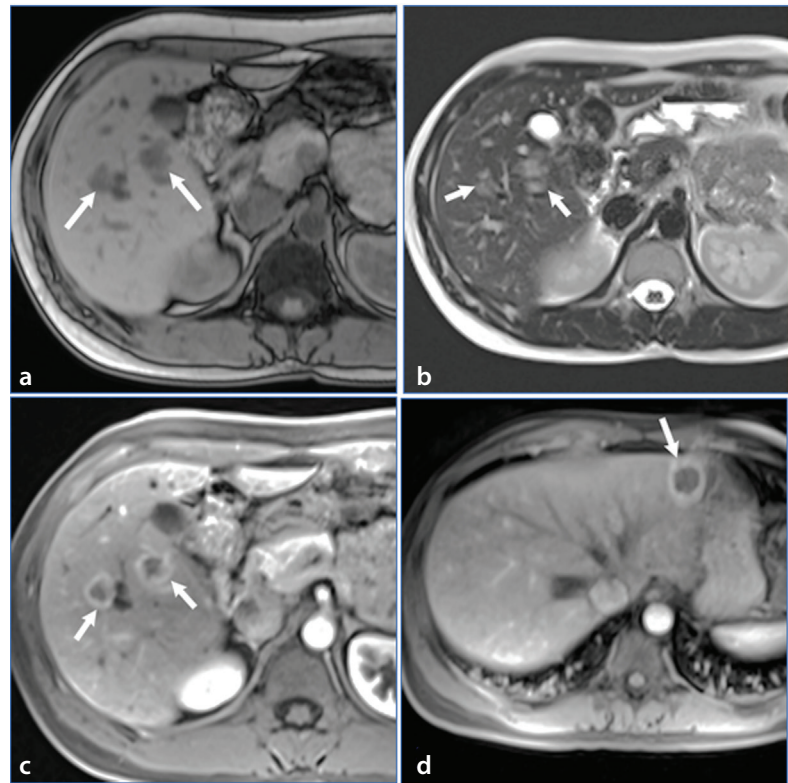


Figure 6. Epithelioid hemangioendothelioma, multiple. Axial T1-weighted (a) and axial T2-weighted (b) images and axial post-gadolinium T1-weighted images with fat suppression (c, d) show multiple liver lesions (arrows). The lesions demonstrate slightly high T2 signal intensity, low T1 signal intensity, and ring-like enhancement following contrast administration.

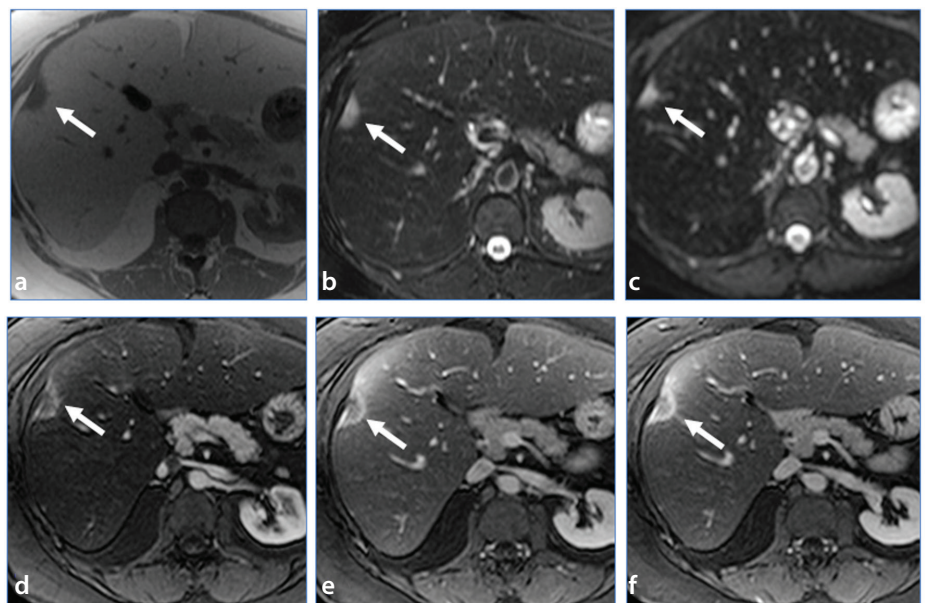


Figure 7. Epithelioid hemangioendothelioma, single. Axial T1-weighted imaging (a), axial T2-weighted imaging with fat suppression (b), axial diffusion-weighted imaging (c), and dynamic post-gadolinium T1-weighted imaging with fat suppression (d-f) show a subcapsular right lobe lesion (arrows) with capsular retraction. The mass demonstrates high T2 signal intensity, low T1 signal intensity, diffusion restriction, and progressive ring-like enhancement following contrast administration.

perintensity and have peripheral enhancement with central areas of patchy irregular enhancement on post-contrast imaging (Figure 8).²⁶ Rarely, these tumors can present with a multicystic appearance, with or without hemorrhage; this is more likely if the tumor is large.²⁵

Schwannoma of the biliary tract can resemble cholangiocarcinoma, and patients may present with jaundice and abdominal pain, a situation that can lead to radiologic misdiagnosis and overtreatment of patients with these tumors.²⁷ Given the concern of biliary obstruction in certain cases, surgical resection is the preferred and curative treatment.²⁸

Multiple myeloma and solitary plasmacytoma

Multiple myeloma is a malignancy of clonal plasma cell proliferation and is the second most common hematologic malignancy. Although plasma cell proliferation generally occurs inside the bone marrow, extramedullary involvement can also be observed. Extramedullary multiple myeloma (EMM) has a reported incidence of 7%–18% at presentation and 6%–20% during disease progression.²⁹ Liver involvement can be seen in up to 34% of patients with EMM. These patients can present with hepatomegaly, jaundice, ascites, and acute liver failure, and tend to have a poor prognosis.²⁹ Imaging features are variable, as EMM can present with a focal mass, multifocal lesions, or diffuse hepatomegaly. On ultrasonography, EMM lesions are usually hypoechoic (Figure 9). On CT, they appear hypoattenuating with mild enhancement, while they may present with low or high signal intensity in T1-weighted images and with a high T2 signal with mild enhancement. On FDG-PET/CT, EMM demonstrates moderate to intense FDG uptake.³⁰

Solitary extramedullary plasmacytoma is a solitary mass of abnormal plasma cells in the absence of systemic myeloma. Hepatic solitary plasmacytoma is rare, and the imaging findings are variable. On FDG-PET/CT, the lesions are hypermetabolic. Patients with solitary plasmacytoma of the liver have a better prognosis than patients with systemic myeloma such as EMM.³¹ Treatment includes autologous stem cell transplant and chemotherapy.

Hepatic lymphoma

Primary hepatic lymphoma (PHL) is an extremely uncommon variant of non-Hodgkin lymphoma (NHL), accounting for

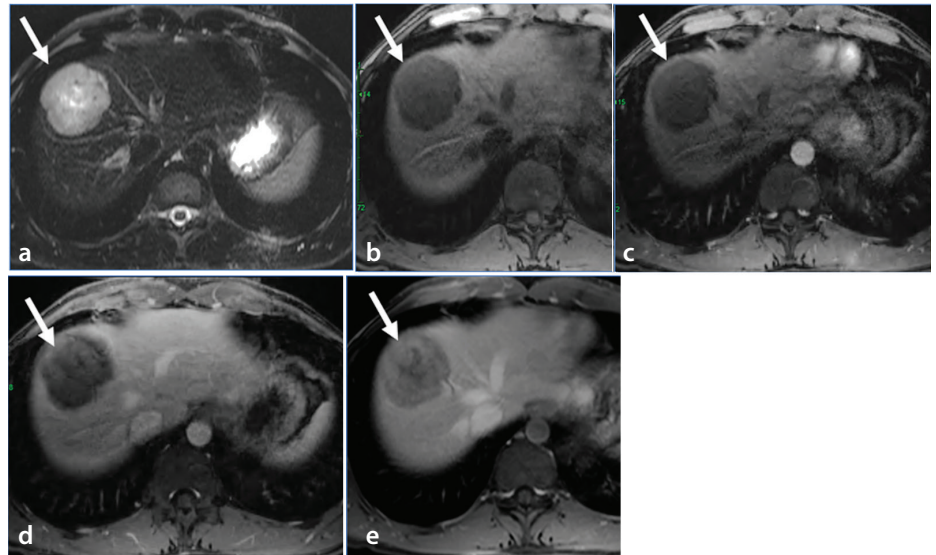


Figure 8. Schwannoma. Axial T2-weighted imaging with fat suppression (a) and dynamic post-gadolinium T1-weighted imaging with fat suppression (b-e) show a right hepatic lobe mass (arrows). The mass demonstrates high T2 signal intensity, low T1 signal intensity, and progressive enhancement following contrast administration.

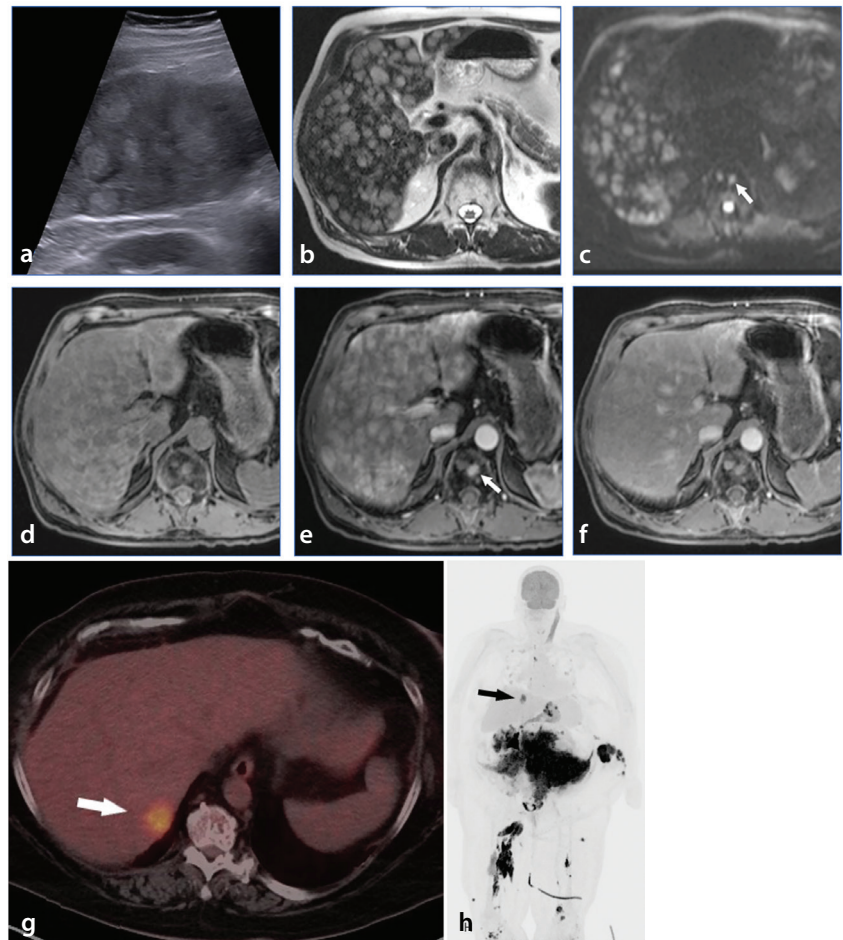


Figure 9. Multiple myeloma. Transabdominal ultrasonography (a) shows multiple hyperechoic liver lesions surrounded by a zone of low echogenicity resulting in target appearance. Axial T2-weighted imaging (b), axial diffusion-weighted imaging (DWI) (c), axial T1-weighted imaging (d), and post-gadolinium T1-weighted imaging with fat suppression during the arterial (e) and delayed (f) phases show numerous liver lesions demonstrating high T2 and low T1 signal intensity, with diffusion restriction on DWI. The lesions show intense enhancement in the arterial phase and are not visible in the delayed phase of contrast enhancement. A fluorodeoxyglucose-positron emission tomography/computed tomography scan (g, h) of a case of extramedullary multiple myeloma shows uptake (white and black arrows).

0.016% of all NHL. PHL is confined to the liver and draining nodes, including the perihepatic and peripancreatic region. Unlike disseminated NHL with liver involvement, PHL shows no evidence of involvement of other visceral organs, distant lymph nodes, or bone marrow for at least 6 months after the onset of hepatic disease; PHL occurs more commonly in men and usually presents in patients in their mid-50s (range: 5–87). Patients may present with abdominal pain, constitutional symptoms, and B symptoms, such as fever and weight loss.³²

The most common presentation of PHL is a solitary mass, while it can also present as multiple masses, and less commonly with diffuse hepatic involvement and a periportal pattern of distribution. On ultrasonography, these lesions are hypoechoic compared with normal liver parenchyma. On CT, the nodules are hypoattenuating with lower enhancement than the surrounding liver. On MRI, the nodules tend to be hypo- or isointense on T1-weighted images and hyperintense on T2-weighted images. Diffusion-weighted MRI is an important component of the imaging protocol due to the highly cellular nature of lymphoma, typically resulting in restricted diffusion in the diffusion-weighted sequences (Figure 10). The PET/CT technique is also helpful in diagnosis, and as with other types of lymphoma, hepatic lymphoma is typically extremely FDG avid.

A distinctive feature is that PHL tumoral masses have an insinuating growth behavior, encasing (not occluding) the vascular structures and bile ducts (Figure 11). Nonetheless, PHL patients are frequently misdiagnosed as having a primary liver tumor or metastatic cancer, and a definitive diagnosis can be achieved through histopathologic examination. Although PHL is an aggressive disease, it is resectable and responsive to chemotherapy and radiotherapy. Therefore, it should be considered in the differential diagnosis for patients presenting with mass lesions in the liver.^{33,34}

Post-transplant lymphoproliferative disorder

Post-transplant lymphoproliferative disorder (PTLD) ranks as the second most common malignancy arising as a complication of solid organ transplant, following non-melanomatous skin cancer.³⁵ It is a disorder related to abnormal lymph node proliferation and encompasses a spectrum of disease processes ranging from benign lymphoid hyperplasia to high-grade malignant lymphomas.³⁶

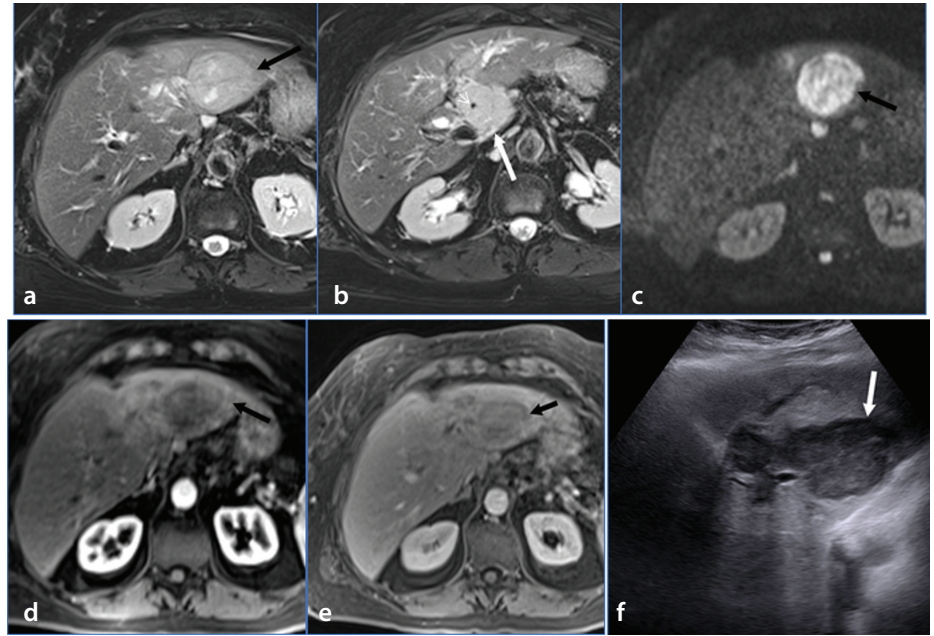


Figure 10. Hepatic lymphoma. Axial T2-weighted imaging (a, b), diffusion-weighted b800 imaging (c), and post-gadolinium T1-weighted imaging with fat suppression during the arterial (d) and delayed (e) phases. There is a well-circumscribed left lobe mass (black arrows) showing heterogeneous increased signal intensity on T2-weighted imaging, diffusion restriction, and poor enhancement following gadolinium administration. The adjacent left lobe demonstrates increased T2 signal intensity due to portal vein compression. A separate mass in the hepatic hilum (long white arrows) shows similar signal and enhancement characteristics. The hilar mass encases the hepatic artery (short white arrow). Transabdominal ultrasonography (f) shows a heterogeneous hypoechoic mass (white arrow).

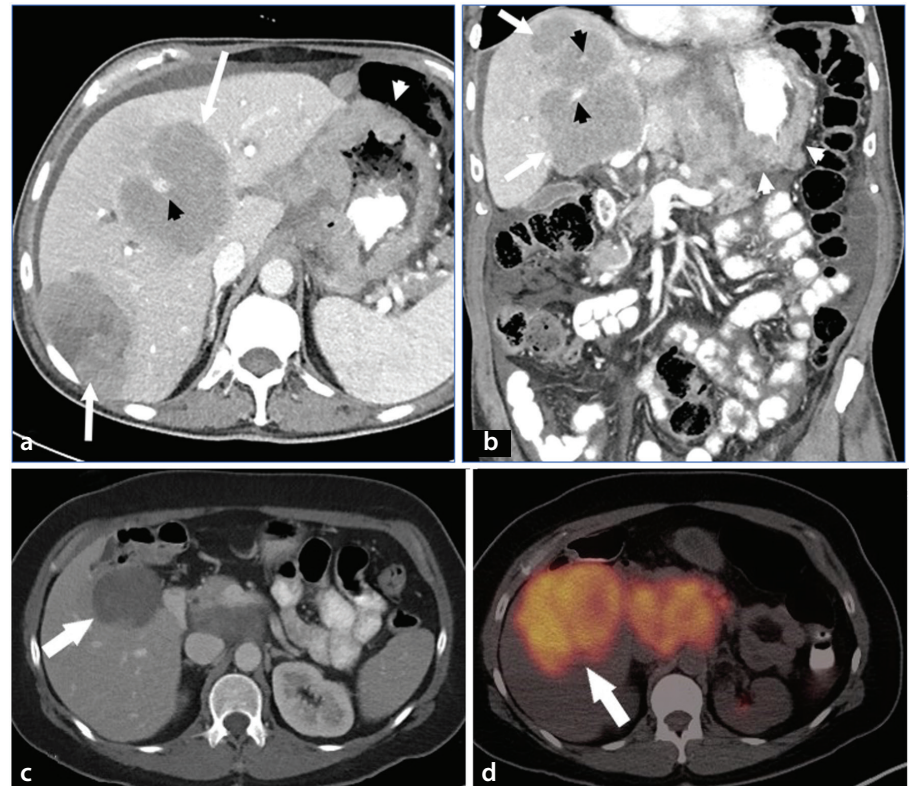


Figure 11. Hepatic lymphoma encasing vessels. Axial (a) and coronal (b) contrast-enhanced computed tomography (CT) shows multiple liver masses (long white arrows) and diffuse gastric wall thickening (short white arrows). As with lymphoma in other parts of the body, hepatic lymphoma tends to encase, rather than occlude, vascular structures. In this case, liver masses appear to encase branches of the portal vein (short black arrows). A companion case demonstrates a contrast enhanced CT scan (c) with a hypoattenuating lymphoma that is markedly fluorodeoxyglucose (FDG) avid on ¹⁸F-FDG-positron emission tomography/CT scan (d) (white arrows).

Epstein-Barr virus (EBV) infection is a significant risk factor for the development of PTLD, particularly in transplant recipients who are EBV-seronegative prior to transplant. Other risk factors include young age, higher levels of immunosuppression following transplant, and having received a liver transplant within the past year.³⁷

The reported incidence of PTLD in liver transplant recipients is variable. Taylor et al.³⁷ reported PTLD in up to 2.8% of adults and up to 15% of children following liver transplant. More recent studies showed a lower incidence of PTLD at 1.5% in adults and 4.3% in the pediatric population.³⁷ Generally, PTLD can be associated with significant morbidity and mortality, particularly in cases of high-grade lymphomas or when the disorder is diagnosed late.³⁵

Unlike lymphoma, PTLD tends to involve extranodal sites such as the liver, and imaging is crucial to its evaluation. Hepatic involvement in PTLD can manifest in different forms and presentations. On CT imaging, PTLD may appear as multiple hypodense masses, a single infiltrating mass, or a heterogeneous mass at the liver hilum causing biliary obstruction (Figure 12). On MRI, the lesion or lesions often have isointense to low signal intensity on T1-weighted images and intermediate to high intensity on T2-weighted images. Dynamic T1-weighted post-contrast images may be characterized by peripheral enhancement, and DWI can show restricted diffusion. However, these imaging features can overlap with those of liver abscesses. This overlap can pose a diagnostic challenge, especially in patients who are at risk for both PTLD and disseminated infections.^{36,38}

Early detection and management of PTLD are critical in improving outcomes for affected individuals. Treatment options such as reducing immunosuppression, antiviral therapy, rituximab (an anti-CD20 monoclonal antibody), chemotherapy, or radiation therapy may be considered depending on the severity and type of PTLD. Regular monitoring for EBV infection can help identify high-risk patients and allow for proactive interventions when necessary.

Hepatic benign cystic teratomas

Teratomas are germ cell tumors that originate from pluripotent cells that have been arrested along their migration pathway. They often contain components derived from all three germ cell layers and present as a cyst with fat, hair, and calcifications. Hepatic benign cystic teratomas are extremely rare, ac-

counting for <1% of all body teratomas. They commonly occur in patients under 3 years old.^{38,39}

Hepatic teratomas are often asymptomatic and may be discovered incidentally during imaging studies for unrelated reasons. However, large tumors can cause symptoms such as abdominal pain, discomfort, or fullness due to compression of neighboring organs. In exceptionally rare cases, hepatic cystic teratomas may rupture.^{38,39}

On CT and MRI, hepatic teratomas typically appear as well-defined cystic lesions with heterogeneous internal components related to variable amounts of fat and calcifications (Figure 13).^{38,39}

Surgical resection is the preferred treatment option for hepatic benign cystic teratomas, especially with large and symptomatic tumors. Complete surgical excision is usually curative, and recurrence is rare following successful resection.³⁹

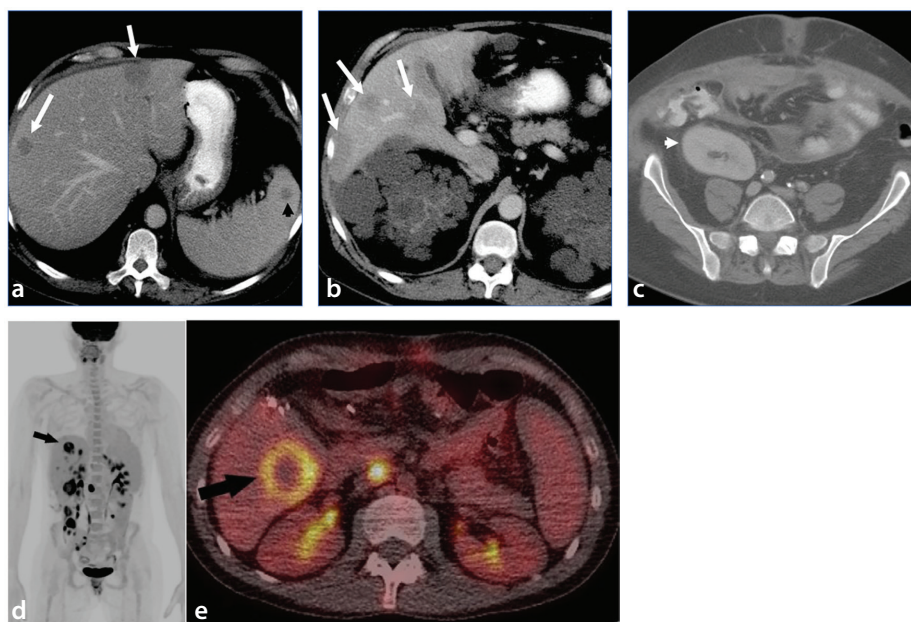


Figure 12. Axial contrast-enhanced computed tomography (CT) images in a 55-year-old man who had undergone renal transplant (short white arrow) 2 years earlier due to autosomal dominant polycystic renal disease and presented with abdominal pain and diarrhea. A contrast-enhanced CT scan (a-c) shows multiple hypoattenuating liver masses (long white arrows) and splenomegaly with one hypoattenuating splenic mass (black arrow). An fluorodeoxyglucose-positron emission tomography/CT scan (d, e) demonstrates uptake (black arrows) in another case of post-transplant lymphoproliferative disorder.

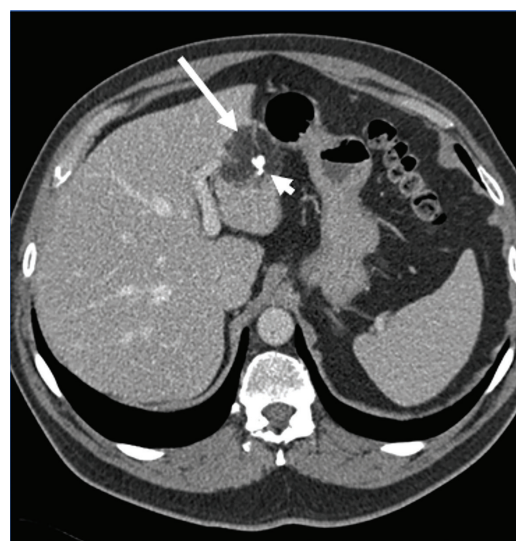


Figure 13. Axial contrast-enhanced computed tomography in the portal venous phase shows a left hepatic lobe mass (long white arrow). The mass was found to represent a teratoma. It is predominantly fatty with peripheral nodular calcifications (short white arrow).

In conclusion, familiarity with the typical appearance of unusual hepatic tumors is important for radiologists. While these tumors are infrequently seen, their inclusion in the differential diagnosis greatly aids the clinician in appropriately triaging patients. This awareness can also avoid unnecessary biopsies, thus improving patient care. This review of several such entities can serve as a useful guide for radiologists in their daily practice.

Acknowledgments

The manuscript was edited by Sarah Bronson, ELS, of the Research Medical Library at The University of Texas MD Anderson Cancer Center.

Conflict of interest disclosure

The authors declared no conflicts of interest.

References

- Tuan Linh L, Minh Duc N, Tu Minh H, et al. Primary hepatic neuroendocrine tumor. *Endocrinol Diabetes Metab Case Rep*. 2021;2021:20-0220. [\[CrossRef\]](#)
- Yang K, Cheng YS, Yang JJ, Jiang X, Guo JX. Primary hepatic neuroendocrine tumors: multi-modal imaging features with pathological correlations. *Cancer Imaging*. 2017;17(1):20. [\[CrossRef\]](#)
- Houat AP, von Atzingen AC, Velloni FG, et al. Hepatic neuroendocrine neoplasm: imaging patterns. *Radiol Bras*. 2020;53(3):195-200. [\[CrossRef\]](#)
- Pan B, Wang SC, Chen ZK, Zou GC. ¹⁸F-FDG-PET/CT findings of a primary hepatic neuroendocrine tumor: a case report and literature review. *J Clin Case Stu*. 2019;5(1). [\[CrossRef\]](#)
- Brazg Ferro L, Wolf I, Peleg Hasson S, et al. Extrapulmonary small cell cancer: a new insight into a rare disease. *Oncology*. 2021;99(6):373-379. [\[CrossRef\]](#)
- Berniker AV, Abdulrahman AA, Teytelboym OM, Galindo LM, Mackey JE. Extrapulmonary small cell carcinoma: imaging features with radiologic-pathologic correlation. *Radiographics*. 2015;35(1):152-163. [\[CrossRef\]](#)
- Crider MH, Hoggard E, Manivel JC. Undifferentiated (embryonal) sarcoma of the liver. *Radiographics*. 2009;29(6):1665-1668. [\[CrossRef\]](#)
- Chung EM, Lattin J, Cube R, et al. From the archives of the AFIP: Pediatric liver masses: radiologic-pathologic correlation. Part 2. Malignant tumors. *Radiographics*. 2011;31(2):483-507. [\[CrossRef\]](#)
- Prasad SR, Wang H, Rosas H, et al. Fat-containing lesions of the liver: radiologic-pathologic correlation. *Radiographics*. 2005;25(2):321-331. [\[CrossRef\]](#)
- Lee SJ, Kim SY, Kim KW, et al. Hepatic angiomyolipoma versus hepatocellular carcinoma in the noncirrhotic liver on gadoxetic acid-enhanced MRI: a diagnostic challenge. *AJR Am J Roentgenol*. 2016;207(3):562-570. [\[CrossRef\]](#)
- Klompshouwer AJ, Dwarkasing RS, Doukas M, et al. Hepatic angiomyolipoma: an international multicenter analysis on diagnosis, management and outcome. *HPB (Oxford)*. 2020;22(4):622-629. [\[CrossRef\]](#)
- Gaballah AH, Jensen CT, Palmquist S, et al. Angiosarcoma: clinical and imaging features from head to toe. *Br J Radiol*. 2017;90(1075):20170039. [\[CrossRef\]](#)
- Yi LL, Zhang JX, Zhou SG, et al. CT and MRI studies of hepatic angiosarcoma. *Clin Radiol*. 2019;74(5):406. [\[CrossRef\]](#)
- Makhlouf HR, Ishak KG, Goodman ZD. Epithelioid hemangioendothelioma of the liver: a clinicopathologic study of 137 cases. *Cancer*. 1999;85(3):562-582. [\[CrossRef\]](#)
- Mehrabi A, Kashfi A, Fonouni H, et al. Primary malignant hepatic epithelioid hemangioendothelioma: a comprehensive review of the literature with emphasis on the surgical therapy. *Cancer*. 2006;107(9):2108-2121. [\[CrossRef\]](#)
- Gan LU, Chang R, Jin H, Yang LI. Typical CT and MRI signs of hepatic epithelioid hemangioendothelioma. *Oncol Lett*. 2016;11(3):1699-1706. [\[CrossRef\]](#)
- Tan H, Zhou R, Yu H, et al. CT appearances and classification of hepatic epithelioid hemangioendothelioma. *Insights Imaging*. 2023;14(1):56. [\[CrossRef\]](#)
- Virarkar M, Saleh M, Diab R, Taggart M, Bhargava P, Bhosale P. Hepatic hemangioendothelioma: an update. *World J Gastrointest Oncol*. 2020;12(3):248-266. [\[CrossRef\]](#)
- Luo L, Cai Z, Zeng S, et al. CT and MRI features of hepatic epithelioid haemangioendothelioma: a multi-institutional retrospective analysis of 15 cases and a literature review. *Insights Imaging*. 2023;14(1):2. [\[CrossRef\]](#)
- Liu X, Yu H, Zhang Z, et al. MRI appearances of hepatic epithelioid hemangioendothelioma: a retrospective study of 57 patients. *Insights Imaging*. 2022;13(1):65. [\[CrossRef\]](#)
- Liu Z, Yi L, Chen J, et al. Comparison of the clinical and MRI features of patients with hepatic hemangioma, epithelioid hemangioendothelioma, or angiosarcoma. *BMC Med Imaging*. 2020;20(1):71. [\[CrossRef\]](#)
- Xu Y, Chen K, Zhang Q, et al. Ultrasound findings of hepatic epithelioid hemangioendothelioma: comparison with other malignant hepatic tumors. *Abdom Radiol (NY)*. 2024;49:762-773. [\[CrossRef\]](#)
- Banerjee B, Rennison A. Epithelioid haemangioendothelioma of liver: a vascular tumour easily mistaken for metastatic carcinoma on ultrasound imaging. *Br J Radiol*. 1992;65(775):611-613. [\[CrossRef\]](#)
- Stacchiotti S, Miah AB, Frezza AM, et al. Epithelioid hemangioendothelioma, an ultra-rare cancer: a consensus paper from the community of experts. *ESMO Open*. 2021;6(3):100170. [\[CrossRef\]](#)
- Haradome H, Woo J, Nakayama H, et al. Characteristics of hepatic schwannoma presenting as an unusual multi-cystic mass on gadoxetic acid disodium-enhanced MR imaging. *Magn Reson Med Sci*. 2018;17(1):95-99. [\[CrossRef\]](#)
- Ota Y, Aso K, Watanabe K, et al. Hepatic schwannoma: imaging findings on CT, MRI and contrast-enhanced ultrasonography. *World J Gastroenterol*. 2012;18(35):4967-4972. [\[CrossRef\]](#)
- Marin Campos C, Garcia Sanz I, Muñoz de Nova JL, Valdés de Anca A, Martín Pérez ME. Schwannoma of the biliary tract resembling cholangiocarcinoma: a case report and review. *Ann R Coll Surg Engl*. 2016;98(7):143-146. [\[CrossRef\]](#)
- Wan DL, Zhai ZL, Ren KW, et al. Hepatic schwannoma: a case report and an updated 40-year review of the literature yielding 30 cases. *Mol Clin Oncol*. 2016;4(6):959-964. [\[CrossRef\]](#)
- Bladé J, de Larrea CF, Rosiñol L. Extramedullary involvement in multiple myeloma. *Haematologica*. 2012;97(11):1618-1619. [\[CrossRef\]](#)
- Tomasian A, Sandrasegaran K, Elsayes KM, Shanbhogue A, Shaaban A, Menias CO. Hematologic malignancies of the liver: spectrum of disease. *Radiographics*. 2015;35(1):71-86. [\[CrossRef\]](#)
- Ng P, Slater S, Radvan G, Price A. Hepatic plasmacytomas: case report and review of imaging features. *Australas Radiol*. 1999;43(1):98-101. [\[CrossRef\]](#)
- Noronha V, Shafi NQ, Obando JA, Kummar S. Primary non-Hodgkin's lymphoma of the liver. *Crit Rev Oncol Hematol*. 2005;53(3):199-207. [\[CrossRef\]](#)
- Ippolito D, Porta M, Maino C, et al. Diagnostic approach in hepatic lymphoma: radiological imaging findings and literature review. *J Cancer Res Clin Oncol*. 2020;146(6):1545-1558. [\[CrossRef\]](#)
- Colagrande S, Calistri L, Grazzini G, et al. MRI features of primary hepatic lymphoma. *Abdom Radiol (NY)*. 2018;43(9):2277-2287. [\[CrossRef\]](#)
- Camacho JC, Moreno CC, Harri PA, Aguirre DA, Torres WE, Mittal PK. Posttransplantation lymphoproliferative disease: proposed imaging classification. *Radiographics*. 2014;34(7):2025-2038. [\[CrossRef\]](#)
- Soliman M, Guys N, Liu P, et al. Multimodality imaging findings of infection-induced tumors.

- Abdom Radiol (NY)*. 2022;47(11):3930-3953. [\[CrossRef\]](#)
37. Taylor AL, Marcus R, Bradley JA. Post-transplant lymphoproliferative disorders (PTLD) after solid organ transplantation. *Crit Rev Oncol Hematol*. 2005;56:155-167. [\[CrossRef\]](#)
38. Borhani AA, Hosseinzadeh K, Almusa O, Furlan A, Nalesnik M. Imaging of posttransplantation lymphoproliferative disorder after solid organ transplantation. *Radiographics*. 2009;29(4):1000-1002. [\[CrossRef\]](#)
39. Ramkumar J, Best A, Gurung A, et al. Resection of ruptured hepatic teratoma in an adult. *Int J Surg Case Rep*. 2018;53:414-419. [\[CrossRef\]](#)